Power Stability Enhancement of SCIG and DFIG Based Wind Turbine Using Controlled-SMES

Hossam S. Salama*‡, I. Vokony**

*Department of Electrical Engineering, Faculty of Engineering, Aswan University, Aswan 81542, Egypt

*Department of Electric Power Engineering, Budapest University of Technology and Economics, Budapest, Hungary

**Department of Electric Power Engineering, Budapest University of Technology and Economics, Budapest, Hungary

(eng.hossam.salah@aswu.edu.eg, vokony.istvan@vet.bme.hu)

‡Corresponding Author; Hossam S. Salama, Department of Electric Power Engineering, Budapest University of Technology and Economics, Budapest, H-1111, Hungary, Tel: +36702533589,

Fax: +36 1 463-3600, eng.hossam.salah@aswu.edu.eg

Abstract- Several installed electrical power systems have a traditional type of wind power (WP) generators called squirrel cage induction generator (SCIG). However, SCIG is not the best type of WP in which it has a harmful impact on the stability of power systems. Therefore, with increase in the loads especially at transient events, the SCIG will lead to system instability. Hence, it is necessary to increase the penetration level of WP by using more efficient generators, such as the doubly-fed induction generator (DFIG). At transient events such as increasing in the loads causes fluctuation of frequency and voltage of power systems. So, it is necessary to use controlled energy storage units to improve the stability of WP. The system used for studying consists of a grid connected to 25 kV bus through a step-down transformer and transmission line supplied initially by SCIG-based WP then supported by DFIG to increase penetration level and covers the increase in the loads. The superconducting magnetic energy storage (SMES) units are proficient in response, efficiency, and lifetime in contrast to another category of energy storage systems, which make it a favored option for renewable energy. If SMES is combined with DFIG and SCIG, it increases the energy capacity of the total system. The SMES-controller is based on fuzzy logic control (FLC). The models of SMES, SCIG-based WP, and DFIG-based WP are demonstrated with MATLAB/SIMULINK, and the results illustrate the success of the proposed control to minimizing the voltage and frequency fluctuations during the transient events. Also, the model illustrates that the performance of DFIG on voltage and frequency stability is better than that of SCIG.

Nomenclature

P_m	Mechanical output power of the wind turbine
C_p	Performance coefficient of the wind turbine
ρ	Air density
R	the radius of the blade
v_{wind}	Wind speed
λ	Tip speed ratio of the rotor
β	Blade pitch angle
E_{SMES}	SMES energy
L_{SMES}	SMES coil inductance
I_{SMES}	SMES coil current
V_{SMES}	SMES coil voltage
P_{SMES}	SMES active power
dI_{SMES}	Change of SMES current
dN_r	Change of SCIG rotor speed

Abbreviations and acronyms

WP	Wind power
SCIG	Squirrel cage induction generator
DFIG	Double fed induction generator
SMES	Superconducting magnetic energy storage
FLC	Fuzzy logic controller
CESS	Controlled energy storage system
RESs	Renewable energy systems
PMSG	Permanent magnet synchronous generator
IGBT	Insulated-gate bipolar transistor
PWM	Pulse width modulation
VSC	Voltage source converter
MFs	Membership functions
PLL	Phase-locked loop

1. Introduction

In 2017, the renewable energy capacity in the world (not including hydropower) is 1081 GW compared 922 GW in 2016. The difference between two recent years is 159 GW, which means the renewable energy sources (RESs) capacity expanded by approximately by 17.2% from 2016 to 2017, indicating huge progress for RESs [1]. The wind energy capacity of 487 GW in 2016 increased to 539 GW in 2017, i.e. wind energy capacity expanded by approximately by 10.7% from 2016 to 2017 [1]. Hence, wind energy is an important and effective renewable energy resource [2]. So, the main target for many countries is growing the RESs production to overcome of increasing in the loads to fully cover the local demand [3] and decreasing the dependency on conventional power plants such as coal [4]. WP have several of the electrical machines topologies, the SCIG is considered one of these topologies, offering advantages such as high reliability, light cost, and low repair requirements. Besides that, slip rings, exciter, or brushes are not necessary for SCIG. So, there is a good investment of SCIG-based WP is still used in the market [5]. But, integration of a SCIG-based WP into the grid affects voltage stability, frequency stability, and transient stability problem more than other WP categories of generators. Although, this type cannot be removed from the system because it will cause a financial loss, so DFIG can be used to facing of increasing in the loads and reduce the bad effect for SCIG on the electrical power system stability.

Compared to the other types, DFIG is widely used in the industry. DFIG is based on a wound-rotor induction generator (WRIG) [6] because it offers the advantages of rugged, high efficiency and energy yield. The DFIG has an acceptable cost and optimum solution. DFIG has a wide operation range of speed because it reaches about one-third of the synchronous speed [7].

Keeping of the electrical power systems at the stable state under abnormal conditions is a very important target for electrical power system requirements hence, the losing of the stable state can lead to a system collapse. The voltage and frequency variations should be kept at permitted limits for improving the voltage and frequency response of power systems. Therefore, the control method for the controlled-energy storage system (CESS) is implemented [8]. The consumers' electricity demand is varying daily or every minute, but the changing of the generated power is a slow process to match the consumer's requirement. The CESSs became a vital part of the electrical power system network wherein, the CESSs can aid the electrical utilities to operate with fixed capacity in presence of the variable load demand and to make the system reliable, secure, and affordable [9]. Therefore, the developments of energy storage systems (ESSs) in the USA and China are considered the largest economy of electricity marketing in the world. In 2015, China has financed collectively capacity of 22.85 GW in ESS, the annual market of ESSs is grew by 243% with additional capacity of 21 GW in the USA [10]. There are

many methods for converting from the traditional energy into a smart grid which utilized the controllable ESSs to preserve the grid requirements. To achieve this goal, ESSs are stored the energy in mechanical form as (Pumped Hydro, flywheel, and Compressed Air), electrochemical form as (Hydrogen Fuel Cell and Batteries), and electrical form as (SMES and supercapacitors).

SMES is using for many power system applications in the future wherein, it is predicted to become a viable choice [11]. In [12], the authors used the SMES and the fault-current limiter based on optimal parameters tuning technique to improve fault-ride-through (FRT) performance and alleviating the output power variation of DFIG connected with the grid. The reference [13] presents a control strategy to mitigate the frequency and voltage fluctuations of a Microgrid during islanding transition. The traditional controller (PID) is used in controlling the SMES energy to improve the power quality of electrical power system equipped with DFIG and permanent magnet synchronous generator (PMSG) of wind turbine [14]. In [15] the authors utilized the controller builds upon the ideas of the well-known direct power control (DPC) for the generator of wind-based of PMSG. The wind turbine power curve is considered one of the important characteristics of the turbine because it is helping in warranty formulations, performance monitoring of the turbines, and energy assessment [16]. The authors in [17] proposed a model based on data partitioning and data mining for modeling power curves of wind turbines to overcome the failure of the turbine with a deteriorating performance. The reference [18] has explained the impact of DFIG and SCIG wind turbine models on small signal stability of the IEEE 14 bus system as a case study.

The authors in [19] have utilized the FLC technique for pitch angle controller of SCIG based WP to maintain the aerodynamic power at its rated value. Theory of the blade element momentum (BEM) is used with tip loss and high thrust corrections to design, optimize and 3D simulation of a small horizontal axis wind turbine rotor [20]. STATCOM is used with SCIG to compensate the reactive power demand for SCIG. The controlled STATCOM with instantaneous reactive power theory [IRPT] control algorithm is applied for the reactive power management [21]. The study of mutual influence among the SCIG based WP and the power system is discussed in [22] where the reactive power has been identified as the more effective option in system design so the reactive power should be controlled, to improve the voltage stability. In [23], the authors have discussed the enhancement of wind generators' rotor speed stability and avoiding the off-line mode from the grid during the abnormal events as well as, compensating the reactive power by using DSTATCOM and dynamic voltage restorer (DVR).

This paper presents the application of DFIG for improving the power system stability in the presence of the SCIG. Wherein, it can be used to increase the penetration level of the generation better than using SCIG only. Also, this paper demonstrates the application of SMES to enhance

the voltage and frequency stability of power systems which fed from SCIG and DFIG wind turbines during transiently load events. By using DFIG and SMES with SCIG, the power system stability can be improved and the overall cost is minimized, wherein, without removing the SCIG from the system, the performance is still more reliable. The SMES active power control technique was achieved by two-quadrant DC-DC chopper using an insulated-gate bipolar transistor (IGBT). A developed FLC is used to determine the duty cycle to control the charging/discharging process of SMES coil through DC-DC chopper. The FLC is selected because of its positive response during abnormal conditions, simplicity, and easy implementation [24]. The proposed control technique of SMES reactive power utilizes PWM and VSC based on PI controllers. The modeling of SCIG, DFIG, SMES system, FLC and PI controllers were performed by Matlab/Simulink® software.

The structure of this paper is summarized as follows. Section 2 introduces the studied system used as a case study. The Modeling of the two types of wind energy is presented in Section 3. Section 4 discusses the modeling of the SMES system. The proposed control method of the SMES is highlighted in Section 5. Section 6 shows the simulation results and analysis. The complete discussions and conclusions are illustrated in Section 7.

2. The Selected Case Study

Figure 1 shows the system which used as a case study during the load transition events. The main components of the system are SCIG-based WP, DFIG-based WP, SMES, and domestic loads. All these components are connected at a common bus, named (BUS) to study the performance of the test system.
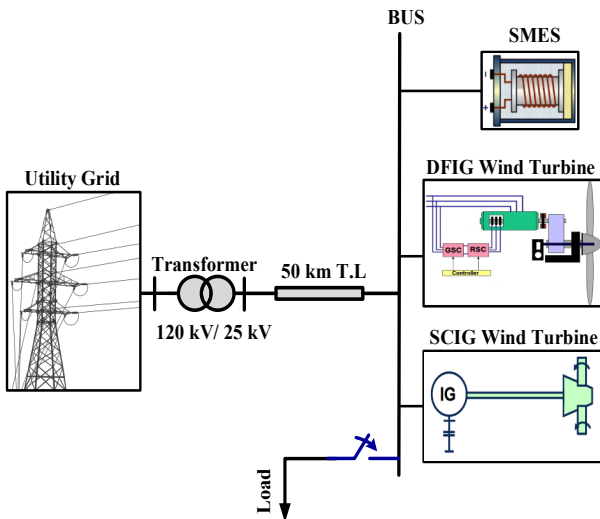

Fig. 1. The configuration of the studied system.

3. Wind Energy System

The WP operation is based on two steps, the first step is the conversion of kinetic energy of the wind speed into mechanical energy. This is due to the aerodynamic rotor

blades actions. The second step is converting the electromechanical power to the electric energy form through the electrical generator. These generators can be divided into four types based on wind power generation concept [25].

The magnitude of wind power depends on the air density ρ (kg/m3) and the wind speed Vw (m/s), as given in equation (1) [26].

$$P_m = 0.5 C_p (\lambda_t, \beta) \pi \, \rho R^2 V^3_w \tag{1}$$

Where P_m is the mechanical power (W); C_p is power coefficient; λ_t is tip speed ratio; β is pitch angle (degree); R is the radius of the blade (m).

3.1. SCIG based on WP

The induction generator can be categorized into several methods [27]. The commonly used model is available in MATLAB/Simulink. In this model, the induction generator of a fixed speed wind turbine is represented by the voltage equation of a SCIG in d-q reference frame. The comprehensive set of the equations (2) to (6) are reported in [28] as shown in Fig. 2 in per unit (pu) system, are [29]. The SCIG parameters are listed in Table 1.
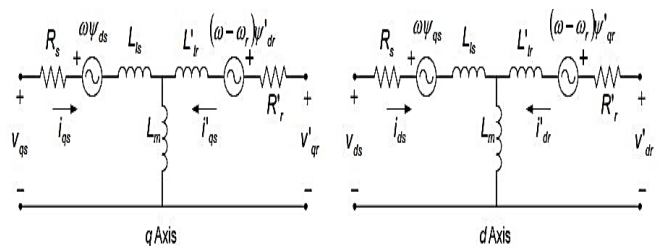

Fig. 2. Model equations of induction generator [29].

$$v_{ds} = R_s i_{ds} + \frac{d\psi_{ds}}{dt} + \omega\psi_{qs} \tag{2}$$

$$v_{qs} = R_s i_{qs} + \frac{d\psi_{qs}}{dt} + \omega\psi_{ds} \tag{3}$$

$$v'_{dr} = 0 = R'_r i_{dr} + \frac{d\psi'_{dr}}{dt} + (\omega - \omega_r)\psi'_{qr} \tag{4}$$

$$v'_{qr} = 0 = R'_r i_{qr} + \frac{d\psi'_{qr}}{dt} + (\omega - \omega_r)\psi'_{dr} \tag{5}$$

$$T_e = \frac{3}{2}p(\lambda_{ds}i_{qs} - \lambda_{qs}i_{ds}) \tag{6}$$

where:

v	voltage (V),
i	current (A),
R_{IG}	resistance of induction generator (Ω),
ψ	the flux (Wb),
d, q	subscripts stand for direct and quadrature component, respectively,
r, s	subscripts for rotor and stator, respectively,
T_e	electrical torque (N.m), and
p	number of pair poles.

Table 1. SCIG parameters

Symbol	Value
S	9/0.9 MVA
V_{rms}	480 V
R_s	0.01965 pu
X_s	0.0397 pu
R_r	0.01909 pu
X_r	0.0397 pu
X_m	1.354 pu
H	0.09526 s
F	0.05479 pu

3.2. The DFIG-WP type

WP based on DFIG consists of a WRIG and an AC/DC/AC converter using IGBT-based PWM. The rotor is connected through the AC/DC/AC converter, but the stator winding is connected directly to the grid. At low wind speeds, the DFIG operation allows to extracting maximum energy by adjusting the turbine speed. The power converter of DFIG is rated at about 30% of the a conventional type wind turbine rated power [30] (i.e. 2.7 MW in this case). During the wind gusts, the DFIG operation helps in minimizing the mechanical stresses on the turbine [31]. The details model of the transient and steady-state stability analysis of DFIG are created. The DFIG parameters are recorded in Table 2.

Table 2. DFIG parameters

Symbol	Value
S	9/0.9 MVA
Vrms	575 V
Rs	0.023 pu
Xs	0.18 pu
Rr	0.016 pu
Xr	0.16 pu
Xm	2.9 pu
H	0.685 s
F	0.01 pu

4. SMES System

In general, the main components of the SMES unit are the superconducting coil, cryogenic system, protection system, power conversion/conditioning system (PCS), and a control system. The method of flowing the dc current through the SMES coil is the main target for SMES design, hence, the charging and discharging process depends on the DC-DC chopper controller. The power transfer from or to the SMES coil depends on the voltage polarity across the coil, as shown in Fig. 3. The DC-DC chopper has three modes; the first one is the charging mode at (Ldi/dt>0), secondly the discharging mode at (Ldi/dt<0), thirdly the standby mode at (Ldi/dt=0).

Equations 7 and 8 express the SMES power (P_{SMES}) and SMES energy (E_{SMES}) by considering a magnet coil

inductance (L_{SMES}). The parameters of the SMES are recorded in Table 3.

$$P_{SMES}=I_{SMES}V_{SMES}=I_{SMES}L_{SMES}(di_{SMES}/dt) \qquad (7)$$

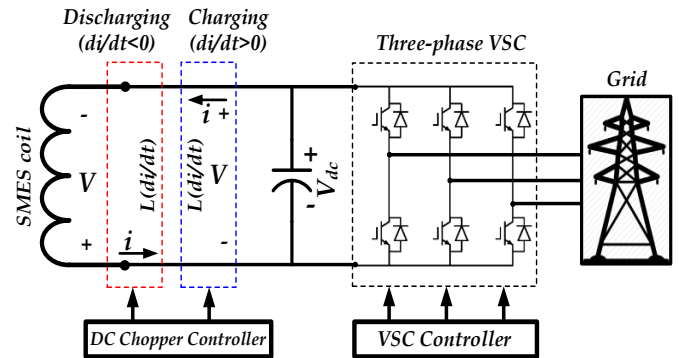$$E_{SMES} = 0.5L_{SMES} I^2_{SMES} \qquad (8)$$

Fig. 3. The component of SMES unit

Table 3. SMES parameters

Symbol	Value
E_{SMES}	2.25 MJ
L_{SMES}	0.5 H
I_{SMES}	3000 A
C_{dc_link}	10 mF

5. The Proposed SMES Control

As shown in Fig. 4, the SMES controller has two main parts, the first part is the voltage source converter (VSC) with its control which used as power electronic interface between the SMES coil and AC side (with 3 MW rated power in this study) and having the two parallel IGBT bridges to reduce the source harmonics. This control depends on traditional control technique (PI control). Fundamentally, a phase-locked loop (PLL) is used to synchronize the VSC with AC side [32]. The AC voltage regulator results of a comparison between AC voltage reference value and AC voltage actual value to produce the quadrature reference current, the DC voltage regulator results of the comparison between DC voltage reference value and DC voltage actual value in order to produce the direct reference current. The current regulator is a comparison between the quadrature reference current and its actual value and the comparison between the direct reference current and its actual value, the extracted value is used to control PWM to pulsate the IGBT.

The second part is the DC-DC chopper and its controller which responsible for Charging/discharging SMES power. This control depends on the FLC as an advanced control technique. Lotfi Zadeh (1965) introduced the FLC technique [33], this technique based on the mathematical tool to overcome the uncertainty issue. FLC technique with soft computing introduces the important impression of computing with words consequently, the treatment of the imprecision

issue. Also, FLC offers a technique for performing linguistic control. Generally, the FLC introduce an inference structure which doing the suitable capability of the human reasoning so, the FLC is adequate for the reasoning approximation, the response is smoother and faster than the conventional technique. In addition, FLC is easy to use and cheaper than the designing model based on the other controller which deal with the same requirements [34]-[35]. The four most common membership functions (MFs) of FLC are shown in [36], the Gaussian MFs is utilized in this study as shown in Fig. 5. The Gaussian curve can be obtained by (9).

$$f(x, \sigma, c) = e^{\frac{-(x-c)^2}{2\sigma^2}} \qquad (9)$$

Where, σ is the parameter indicates the width of the curve, and c parameter is located the distance from the origin. Wherein, the steps of designing FLC for DC-DC chopper can be showed in the following stages: (i) Determine and state the inputs and output that should be reached, as shown in Fig. 4. The FLC has two input and one output, the first input is the SCIG rotor speed deviation (dN_r), which is the difference between the reference rotor speed and the actual rotor speed, also it has five sets of Gauss-type MFs as presented in Fig. 5 with replacing

X to dNr named as (NL = Negative Large, NS = Negative Small, Z = Zero, PS = Positive Small, PL = Positive Large). By similarity, the other input is the SMES current deviation (dI_{SMES}), it is the difference of SMES reference and actual current. Also, the MFs of the second input can be named as (NL = Negative Large, NS = Negative Small, Z = Zero, PS = Positive small, PL = Positive Large), the output of the FLC is duty cycle (D) the MFs can be itemed as (CS = Charge Small, CL = Charge Large, DS = Discharge Small, DL = Discharge Large, SB =Standby). (ii) Design rules based on the state of the FLC inputs which can be used under any conditions. This can be easier if the design of the rules base in the true table model as recorded in Table 4. (iii) Determine the statement which should be used to transform fuzzy control rules into crisp control actions, the statement used in this study is (IF–AND–THEN). This is also part of the defuzzification stage of the fuzzy output. The FLC output signal is compared with a sawtooth signal to produce the required pulses for the DC-DC chopper switches. This, in turn, can be achieved to apply a positive voltage (S_1 and T_S are on), in the charging process (i.e. D > 0.5) or negative voltage (S_1 and S_2 are off) in the discharging process (i.e. D < 0.5) or zero voltage (D_1 and S_1 are on) in case of the standby process of the SMES coil, that is means the duty cycle is equal to 0.5.
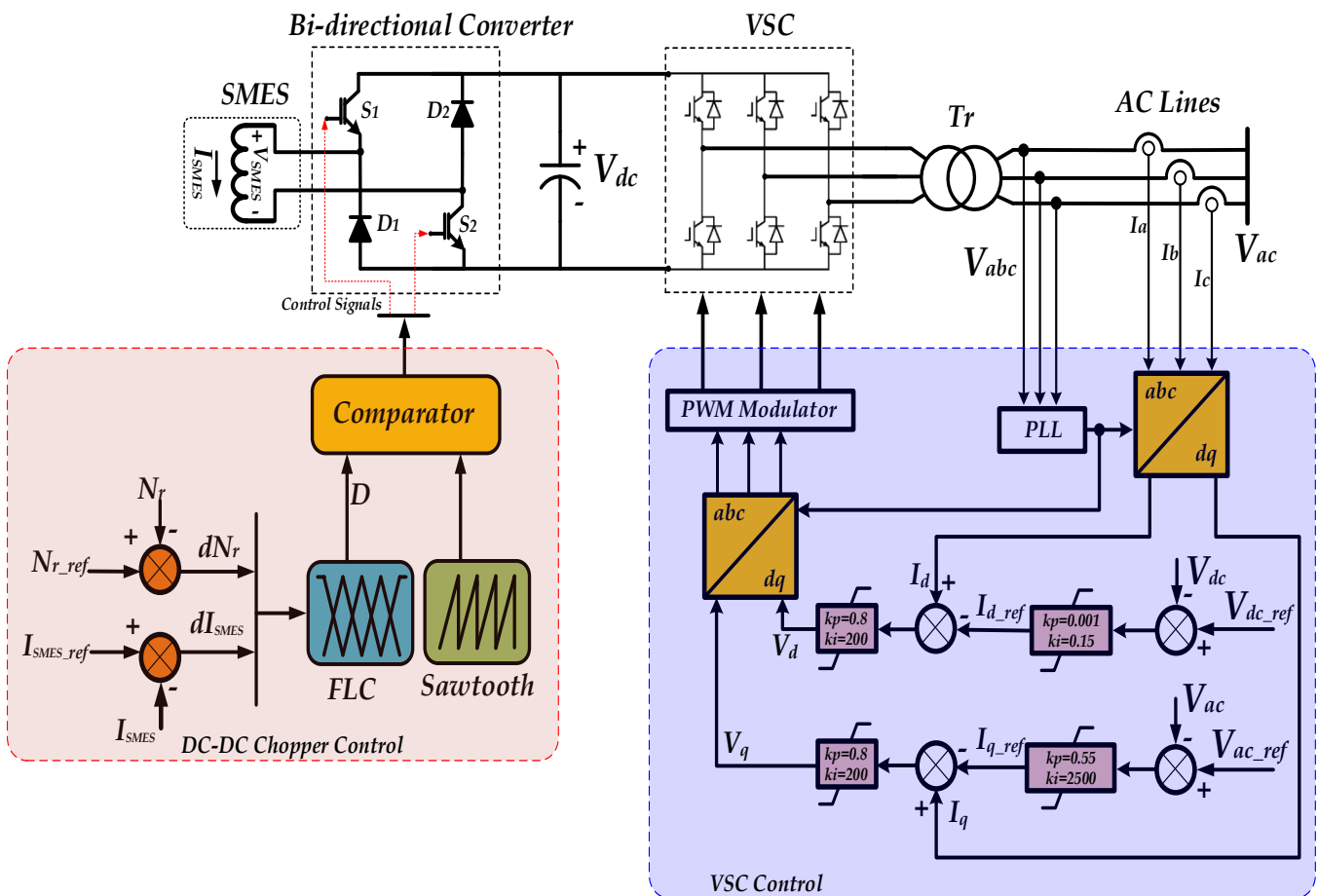

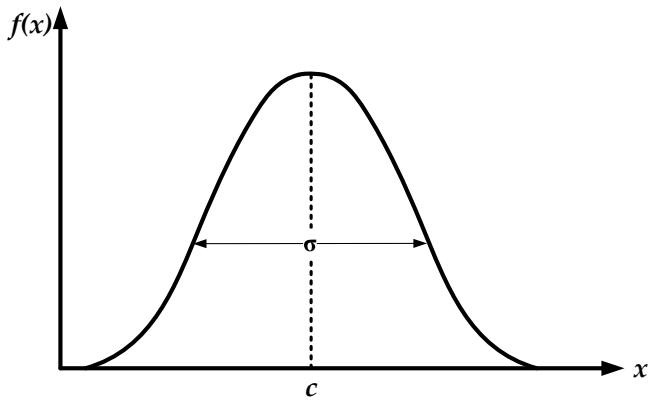**Fig. 4.** The complete control of the DC-DC chopper and VSC.

Fig. 5. The Gaussian curve for input and output variables.

Table 4. Fuzzy logic SMES rules

dISMES	dNr				
	NL	NS	Z	PS	PL
NL	SB	SB	SB	SB	SB
NS	CS	SB	SB	DL	DL
Z	CL	CS	SB	DS	DL
PS	CL	CL	CS	SB	DS
PL	CL	CL	CS	SB	DS

6. Results and Analysis

To indicate the impact of DFIG and controlled-SMES on the power system stability in the presence of SCIG, the load can be connected and disconnected according to the scenario which highlighted in Table 5. The wind speed is assumed to be constant. Therein, the DFIG and SMES systems are connected to the power network to compensate the load demand and improving the power system stability as well as the SCIG performance. Fig. 6.a, b, and c indicate the variables of FLC (dV_w, dI_{smes}, and D) which are fuzzified into five sets of Gaussmf-type membership functions (MFs). dV_w, dI_{smes}, and D have variation ranges to develop a set of fuzzy logic rules. Fig. 6.d illustrates a three-dimensional (3-D) visualization of the control space. The surface viewer shows the inputs and output relation.

Table 5. The scenario of load state

Load connection	t(s)=3
Load disconnection	t(s)=4

(a)

(b)

(c)

(d)

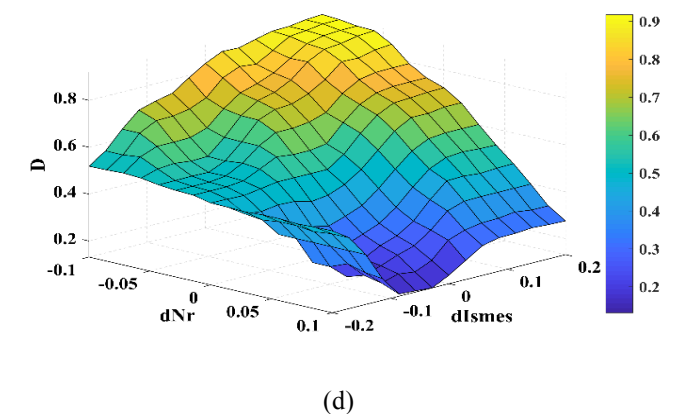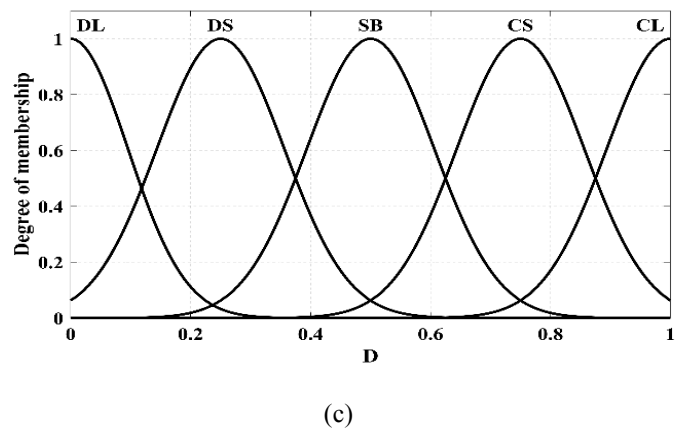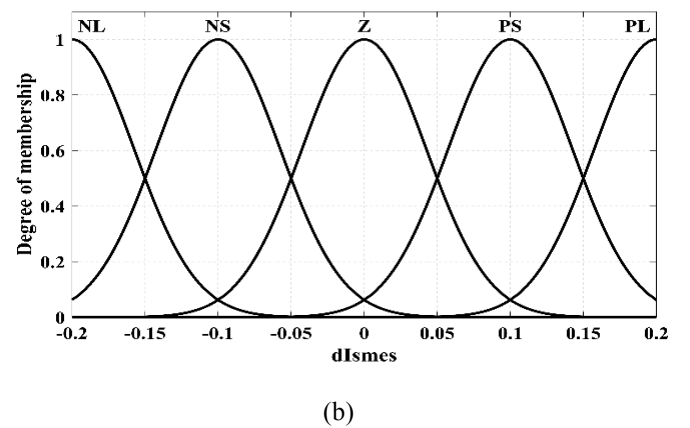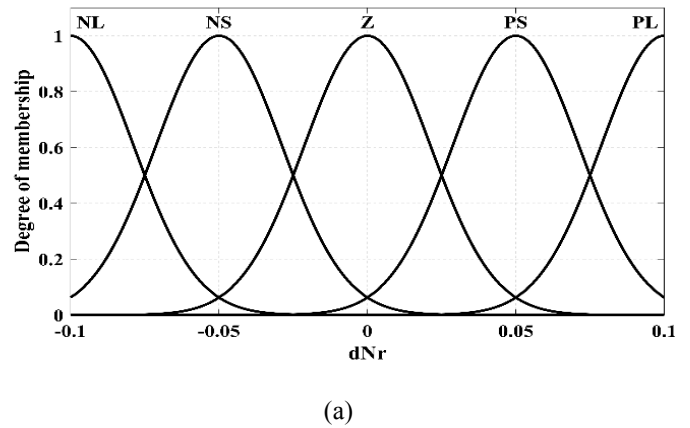**Fig. 6.** MFs for: (a) dNr, (b) dIsmes, (C) D, (d) and relation between inputs and output in 3-D

Fig. 7. shows the voltage response at the common point BUS, it seems that during the transient event (load connection and load disconnection), the voltage value dropped to approximately 0.875 pu in the case of SCIG only while it is regulated to 0.95 pu after connecting the DFIG to the system. After installing SMES, the voltage is mitigated to 0.99 pu approximately. SMES and DFIG can be used to reduce the value of overshoot and undershoot fluctuation of frequency deviation as shown in Fig. 8. The oscillations of SCIG speed are fastly damped by using the SMES with DFIG and SGIG, as shown in Fig. 9. Figs. 10 and 11 present the response of SMES reactive and active powers, respectively. SMES can inject the reactive power to compensate the voltage variation and for supplying the required reactive power to the SCIG as well. Also, SMES active power can be changed positively and negatively to damp effectively the oscillation in the system frequency, as shown in Fig. 10.
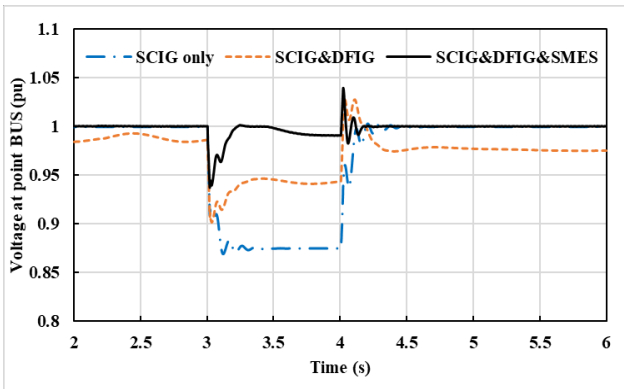
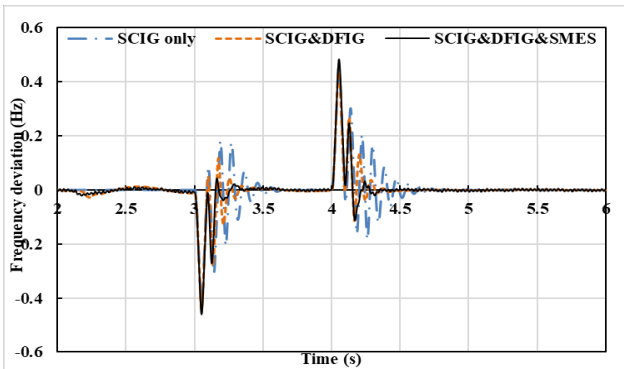

Fig. 7. Voltage response at point "BUS".

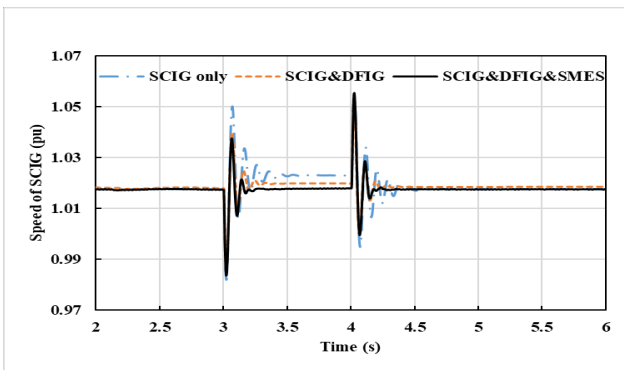**Fig. 8.** The frequency deviation response.
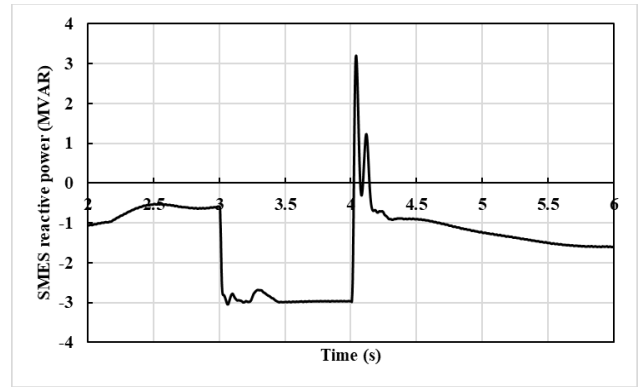

Fig. 9. SCIG speed variation.

Fig. 10. SMES reactive power response.

The response of the duty cycle of the chopper circuit is discussed in Fig. 12. It can be seen that the value of the duty cycle changes less than or greater than 0.5 according to discharging and charging modes, respectively. This, in turn, helps in mitigating the voltage variation as well as rapidly damping in the frequency oscillations. The response of the voltage across the SMES coil which has a positive, negative or zero according to the SMES modes as shown in Fig. 13. Furthermore, the SMES current and SMES energy response are presented in Figs. 14 and 15 respectively. Finally, Fig. 16 shows the response of the DC-linked voltage which linked between the chopper circuit and the VSC. The value of the voltage is regulated to an approximately constant value at 2400 V during all modes of the SMES operation, this can prove and validate of the robustness and the reliability of the proposed control method.
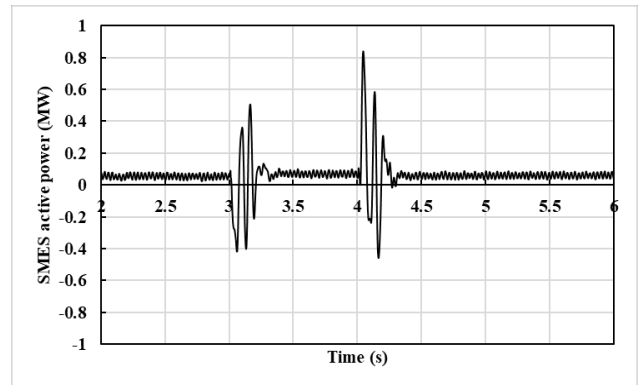

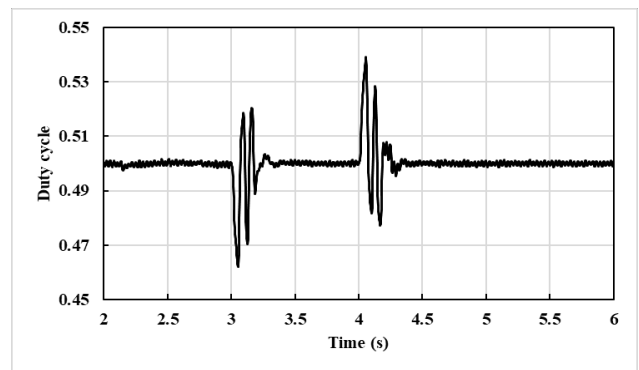
Fig. 11. The behavior of SMES active power.
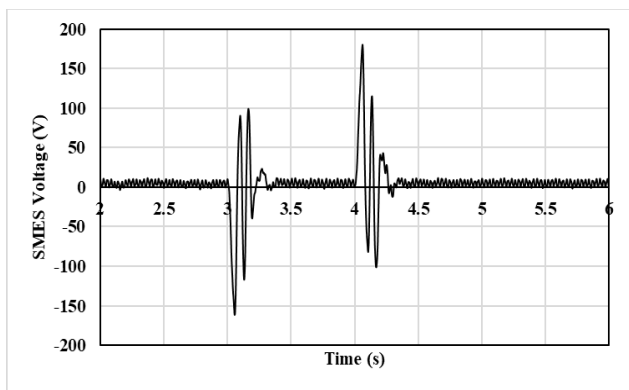

Fig. 12. The duty cycle performance.
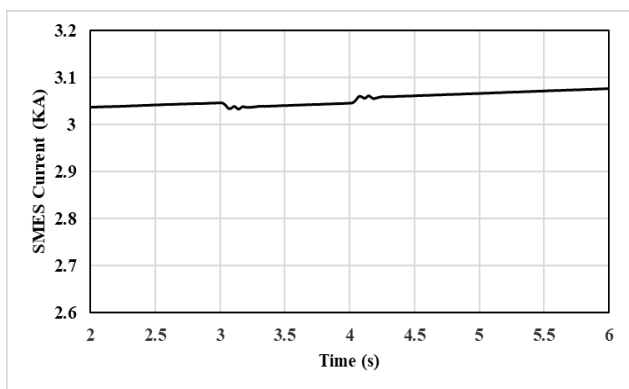
153

Fig. 13. SMES Voltage
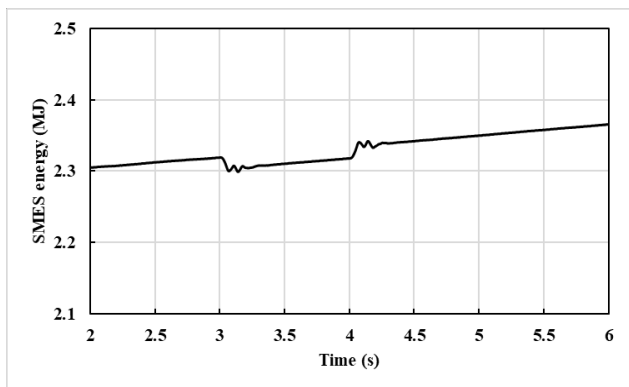

Fig. 14. SMES Current
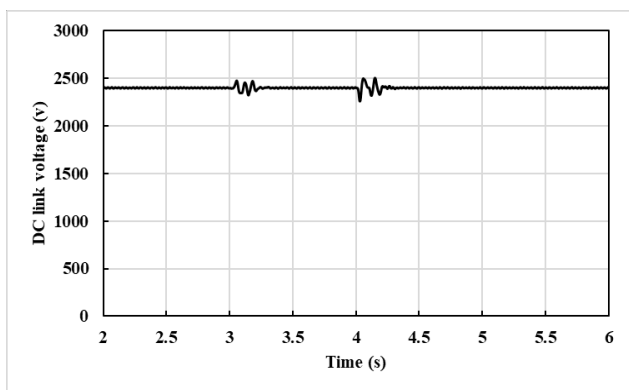

Fig. 15. SMES energy response.

Fig. 16. The DC link voltage.

7. Conclusion

This paper has presented an effective control technique to improve the stability of the power system. Furthermore, the SCIG performance has been enhanced by installing the DFIG and controlled-SMES. The SMES energy is controlled by FLC applied to the bi-directional dc-dc converter of a SMES unit. FLC using two inputs; the SCIG rotor speed deviation and the SMES current deviation. SMES is controlled maintained at standby mode during the normal operation of the system, otherwise, charge /discharge its stowed energy during irregular events could occur in the system such as load insertion/removal. The main contributions that can be summarized from this case-study are, the proposed FLC applied to the SMES succeed to maintain the stability of the system. Moreover, the PI control strategy was used to control the reactive power transfers from the SMES. Using the proposed control method, both the BUS point voltage and frequency are improved during load insertion/removal events.

In general, the SCIG has low cost and simple construction, therefore, the combining of DFIG and SMES is considered the best solution to improve the SCIG performance. Finally, this concept can gather between the economical solution and the better performance of the power system operation.

References

[1]   Renewable Energy Policy Network for the 21st Century, Renewables Global Status Report (GSR), REN21, 2018.

[2]   A. Harrouz, M. Abbes, I. Colak, and K. Kayisli, "Smart grid and renewable energy in Algeria" , IEEE 6th International Conference on Renewable Energy Research and Applications (ICRERA), San Diego, CA, USA, pp. 1166–1171, 5-8 Nov. 2017.

[3]   D. Motyka, M. Kajanova, and P. Bracinik, "The Impact of Embedded Generation on Distribution Grid Operation" , IEEE 7th International Conference on Renewable Energy Research and Applications (ICRERA), Paris, France, pp. 360–364, 14-17 Oct. 2018.

[4]   P. Mazidi, G. N. Baltas, M. Eliassi, and P. Rodriguez, "A Model for Flexibility Analysis of RESS with Electric Energy Storage and Reserve" , 7th International Conference on Renewable Energy Research and Applications (ICRERA), Paris, France, pp. 1004–1009, 14-17 Oct. 2018.

[5]   U. Eminoglu, "A New Model for Wind Turbine Systems" , Electr. Power Components Syst., vol. 37, no. 10, pp. 1180–1193, Sep. 2009.

[6]   A. Beainy, C. Maatouk, N. Moubayed, and F. Kaddah, "Comparison of different types of generator for wind energy conversion system topologies" , 3rd International Conference on Renewable Energies for Developing Countries (REDEC), Zouk Mosbeh,

Lebanon, pp. 1–6, 13-15 July 2016.

[7]   N. Kumar, T. R. Chelliah, and S. P. Srivastava, "Analysis of doubly-fed induction machine operating at motoring mode subjected to voltage sag" , Eng. Sci. Technol. an Int. J., vol. 19, no. 3, pp. 1117–1131, Sep. 2016.

[8]   T. Morstyn, B. Hredzak, and V. G. Agelidis, "Control Strategies for Microgrids With Distributed Energy Storage Systems: An Overview" , IEEE Trans. Smart Grid, vol. 9, no. 4, pp. 3652–3666, Jul. 2018.

[9]   J. Song, S. J. Song, S.-D. Oh, and Y. Yoo, "Optimal operational state scheduling of wind turbines for lower battery capacity in renewable power systems in islands" , 5th IEEE International Conference on Renewable Energy Research and Applications (ICRERA), Birmingham, UK, pp. 164–168, 20-23 Nov. 2016.

[10]   Y. Zhang *et al.*, "Grid-Level Application of Electrical Energy Storage: Example Use Cases in the United States and China" , IEEE Power Energy Mag., vol. 15, no. 5, pp. 51–58, Sep. 2017.

[11]   F. Mohamad *et al.*, "Development of Energy Storage Systems for Power Network Reliability: A Review" , Energies, vol. 11, no. 9, p. 2278, Aug. 2018.

[12]   I. Ngamroo, "Optimization of SMES-FCL for Augmenting FRT Performance and Smoothing Output Power of Grid-Connected DFIG Wind Turbine" , IEEE Trans. Appl. Supercond., vol. 26, no. 7, pp. 1–5, Oct. 2016.

[13]   H. S. Salama, M. Abdel-Akher, and M. M. Aly, "Development energy management strategy of SMES-based Microgrid for stable islanding transition" , 18th IEEE International Middle East Power Systems Conference (MEPCON), Cairo, Egypt, pp. 413–418, 27-29 Dec. 2016.

[14]   M. A. A. Khan, M. M. Shahriar, and M. S. Islam, "Power Quality Improvement of DFIG and PMSG Based Hybrid Wind Farm Using SMES" , 2nd International Conference on Electrical & Electronic Engineering (ICEEE), Rajshahi, Bangladesh, pp. 1–4, 27-29 Dec. 2017.

[15]   A. Harrouz, I. Colak, and K. Kayisli, "Control of a small wind turbine system application" , 5th IEEE International Conference on Renewable Energy Research and Applications (ICRERA), Birmingham, UK, pp. 1128–1133, 20-23 Nov. 2016.

[16]   V. Sohoni, S. C. Gupta, and R. K. Nema, "A critical review on wind turbine power curve modelling techniques and their applications in wind based energy systems" , Journal of Energy, vol. 2016, pp. 1-19, 2016.

[17]   T. Ouyang, A. Kusiak, and Y. He, "Modeling wind-turbine power curve: A data partitioning and mining approach" , Renewable Energy, vol. 105, pp.1-8, 2017.

[18]   D. R. Chandra et al., "Impact of SCIG, DFIG wind power plant on IEEE 14 bus system with small signal stability assessment" , 18th National Power Systems Conference (NPSC), Guwahati, India, pp. 1–6, 18-20 Dec. 2014.

[19]   K. A. Naik and C. P. Gupta, "Fuzzy logic based pitch angle controller/or SCIG based wind energy system" , Recent Developments in Control, Automation & Power Engineering (RDCAPE), Noida, India, pp. 60–65, 26-27 Oct. 2017.

[20]   M. Magri, A. Raihani, A. El Magri, A. El Fadili, and M. El Youssfi, "Aerodynamic design and 3D analysis of wind turbine rotor" , Renewable Energies, Power Systems & Green Inclusive Economy (REPS-GIE), Casablanca, Morocco, pp. 1–6, 23-24 April 2018.

[21]   K. J. Aparna, M. R. Sindhu, and M. Jisma, "Reactive power management of a grid connected SCIG using STATCOM" , International Conference on Circuit ,Power and Computing Technologies (ICCPCT), Kollam, India, pp. 1–5, 20-21 April 2017.

[22]   A. Edrisian, A. Goudarzi, M. Ebadian, A. G. Swanson and D. Mahdiyan, "Assessing the Effective Parameters on Operation Improvement of SCIG based Wind Farms Connected to Network" , International Journal of Renewable Energy Research. Vol. 6, no. 2, pp. 1-8, 2016.

[23]   V. M. Hrishikesan, K. Venkatraman, and M. P. Selvan, "Performance of custom power devices in SCIG based Wind farms during abnormal grid conditions" , Annual IEEE India Conference (INDICON), Pune, India, pp. 1–5, 11-13 Dec. 2014.

[24]   S. Saad and L. Zellouma, "Fuzzy logic controller for three-level shunt active filter compensating harmonics and reactive power" , Electr. Power Syst. Res., vol. 79, no. 10, pp. 1337–1341, Oct. 2009.

[25]   E. H. Camm et al., "Wind power plant collector system design considerations: IEEE PES wind plant collector system design working group" , IEEE Power & Energy Society General Meeting, Calgary, AB, Canada, pp. 1–7, 26-30 July 2009.

[26]   C. Abbey, F. Khodabakhchian, N.-M. Zhou, S. Dennetière, M. J. Mahseredjian, and G. Joos, "Transient Modeling and Comparison of Wind Generator Topologies" , International Conference on Power Systems Transients (IPST'05), Montreal, Canada, pp. 19-23, June 2005.

[27]   S. Heier, Grid integration of wind energy, John Wiley & Sons, 2014.

[28]   T. Ackermann, Wind power in power systems, John Wiley & Sons, 2005.

[29]   F. González-Longatt, Omar Aymaya, Marco Cooz and Luis Duran, "Dynamic behavior of constant speed wt based on induction generator directly

connected to grid" , 6th World Wind Energy Conference and Exhibition (WWEC), Argentina, Oct. 2007.

[30] E. Muljadi, M. Singh, and V. Gevorgian, "Doubly Fed Induction Generator in an Offshore Wind Power Plant Operated at Rated V/Hz" , IEEE Trans. Ind. Appl., vol. 49, no. 5, pp. 2197–2205, Sep. 2013.

[31] F. M. Hughes, O. Anaya-Lara, N. Jenkins, and G. Strbac, "Control of DFIG-Based Wind Generation for Power Network Support" , IEEE Trans. Power Syst., vol. 20, no. 4, pp. 1958–1966, Nov. 2005.

[32] T. Thacker, D. Boroyevich, R. Burgos, and F. Wang, "Phase-Locked Loop Noise Reduction via Phase Detector Implementation for Single-Phase Systems" , IEEE Trans. Ind. Electron., vol. 58, no. 6, pp. 2482–2490, Jun. 2011.

[33] L.A. Zadeh, "Fuzzy Sets" , Information and control 8, no. 3, pp. 338-353, 1965.

[34] J. Y. M. Cheung, "Fuzzy logic control of refrigerant flow" , UKACC International Conference on Control. Control '96, vol. 1, Exeter, UK, pp. 125–130, 2-5 Sept. 1996.

[35] L. Dambrosio, "Data-based Fuzzy Logic Control Tenchnique Appied to a Wind System" , Energy Procedia, vol. 126, pp. 690–697, Sep. 2017.

[36] Zhao, Jin, and Bimal K. Bose, "Evaluation of membership functions for fuzzy logic controlled induction motor drive" , IECON-proceedıngs-. Vol. 1. pp. 229-234, Nov. 2002.